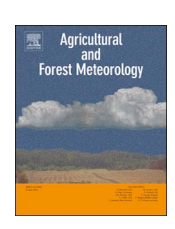
FISEVIER

Contents lists available at ScienceDirect

Agricultural and Forest Meteorology

journal homepage: www.elsevier.com/locate/agrformet



Geospatial coherence of surface-atmosphere fluxes in the upper Great Lakes region



Jeralyn Poe^{a,b}, David E. Reed^{a,c,*}, Michael Abraha^a, Jiquan Chen^a, Kyla M. Dahlin^a, Ankur R. Desai^d

- ^a Michigan State University, Department of Geography, Environment, and Spatial Sciences, East Lansing MI, USA
- Deliant Northern Arizona University, School of Informatics, Computing, and Cyber Systems, Flagstaff, AZ 86011, USA
- ^c University of Science and Arts of Oklahoma, Environmental Science, Chickasha, OK 73018, USA
- ^d University of Wisconsin Madison, Department of Atmospheric and Oceanic Sciences, Madison WI, USA

ARTICLE INFO

Keywords: Spatial coherence Eddy covariance Empirical orthogonal function Spatial scaling Midwestern USA

ABSTRACT

Surface-atmosphere fluxes are known to vary at multiple time scales, but uncertainty is high as to how fluxes change spatially within regions. With an increase in the number of eddy covariance towers, we are now able to examine the geospatial coherence of ecosystem fluxes, using time-series correlation. Eighteen sites from Michigan and Wisconsin were used in this study, ranging from 100 m to 600 km apart. Surface-atmosphere fluxes from a six-month period were used to quantify spatial coherence on a pair-wise basis. Using geospatial statistics, carbon and sensible heat (H) fluxes were found to be 95% correlated directly outside of their flux footprint and 56% correlated up to a distance of \sim 35 km. Latent (LE) and momentum (τ) fluxes were less correlated, 83% directly outside of their flux footprint and 40% at a distance of ~130 km albeit, at a much larger spatial distance than for the carbon and sensible heat fluxes. All fluxes showed strong spectral resonance at diel and seasonal timescales, with 1-, 2- and 3-month periods being common modes of variability among H, LE, and τ fluxes. Results based on Empirical Orthogonal Function show distinct transitions of net ecosystem exchange from fall to winter before photosynthesis or respiration while H and τ do not exhibit coherent trends. This work demonstrates the potential of quantifying geospatial coherence of surface-atmosphere fluxes in the Midwestern United States, with the ability to predict fluxes beyond the spatial limit of a single flux tower footprint. Ultimately, expanding the flux measurements to larger scales would allow better spatial scaling of terrestrial surface-atmosphere fluxes between tower footprint and modeling or remote sensing scales.

1. Introduction

Interactions between the land surface and the atmosphere have substantial implications for regional and global climate and changes. Land cover changes impact mass and energy exchanges between the surface and the atmosphere, particularly the water, greenhouse gas and energy at local to regional scales (Bounoua et al., 2002). Accurate parametrization of land-surface models to explicitly represent mass and energy exchange processes remains a challenge (Bonan, 1995; Xiao et al., 2014; Xiao et al., 2011). To this end, accurate surface-atmosphere flux observations are crucial to constrain these exchange processes in order to reduce the source of uncertainty in land-surface models.

Developing networks of surface-atmosphere flux observations, while critical, is costly and challenging. Instrumentation for direct

observations using eddy covariance (EC) and mesoscale networks cost at least \$45,000 per site (Billesbach et al., 2004) and often require a high degree of technical knowledge/skills to operate. Remotely sensed products and models need observational data for ground truthing and model parametrization (Wu et al., 2010; Xiao et al., 2014) — justifying the need for surface-atmosphere flux observations (Baldocchi, 2014). However, the footprints of surface-atmosphere flux observations are spatially small, requiring an array of stations to adequately cover biomes in a range of geographical locations and climates to quantify landscape and regional fluxes. For example, an 82-m tall tower over a forest with roughness length varying from 0.1 m to 0.4 m has only a 1-km radius ground-area footprint (Barcza et al., 2009). These issues pose a challenge of upscaling surface-atmosphere fluxes which have been an active research area for decades (Baldocchi, 2014; Baldocchi et al., 1991; Xiao et al., 2014; Desai et al., 2008).

E-mail address: david.edwin.reed@gmail.com (D.E. Reed).

^{*} Corresponding author.

Previous scaling methods have focused on scaling from flux observations (1 km scale) to satellite pixel scales (1-10 km scale for medium resolutions) or model grid scales (10-100 km) (Liu et al., 2016). Over the last four decades, there have been a number of multisite field campaigns that compared ground-based EC observations to remote sensing estimation methods and model simulations. Among these field campaigns are: the First ISLSCP (International Satellite Land Surface Climatology Project) Field Experiment Sellers et al. (1988)), the Northern Hemisphere Climate Processes Land-Surface Experiment (NOPEX; Halldin et al. (1999)), and the Lindenberg Inhomogeneous Terrain-Fluxes between Atmosphere and Surface: a Long-term Study (LITFASS-98; Beyrich et al. (2002)), HiWater MUSO-EXE (Liu et al., 2016; Ran et al., 2016) and LITFASS-2003; Beyrich and Mengelkamp (2006). These field campaigns have used a number of scaling methods, including arithmetic averages (Shuttleworth et al., 1989), area weighted methods (Beyrich et al., 2006), numerical models (Heinemann and Kerschgens, 2005), and geospatial analysis (i.e., spatial statistics, modeling). With one of the most spatially dense multisite field campaigns, Ge et al. (2015) and Liu et al. (2016) used flux observations from 17 EC sites within a 5.5 km by 5.5 km study area to upscale between multiple surface-atmosphere flux methods using geospatial Kriging. However, we seek to extend the spatial scales farther than 5.5 km, and explicitly test the spatial coherence of fluxes as a function of distance, in order to ultimately upscale fluxes from single footprint to regional scale.

The concept of spatial coherence across a landscape is well studied in terrestrial ecosystem studies (Cleland et al., 2007; Badeck et al., 2004), but has rarely been applied to research on land-surface fluxes. Desai (2010) shows a spatial coherence of interannual variability from carbon fluxes and phenological drivers and concludes that models operating at 100 km grid scales could extrapolate climate-phenological relationships to model interannual carbon cycling. Coherent behavior of surface-atmosphere fluxes was found between sites with similar surface-atmosphere fluxes, with time-varying similarities of aerodynamic canopy height founds between forested and grassland sites (Chu et al., 2018). More explicitly focused on surface-atmosphere fluxes, Hollinger et al. (2004) examined coherence between two towers ~775 m apart and found the annual sums of net carbon fluxes to be within 6% of each other, and model parameters derived from observations were not significantly different, showing that for modeling purposes, the two sites were identical. Following these studies, we hypothesize surface-atmosphere fluxes to be spatially coherent to each other, but with an unknown coherence at scales between 1 and 100 km.

In order to extrapolate observations beyond the footprint of a single EC tower to the landscape, first data from multi-sites was used to test for similarity across increasing spatial distances. Here, we use six months of surface-atmosphere flux data from two clusters of flux sites and eighteen sites. We seek to answer the following research questions:

1) Is there a geospatial relationship between signal coherence of surface-atmosphere fluxes? 2) To what spatial extent does a single coherence exist for surface-atmosphere fluxes? and 3) Do these fluxes have common frequencies of variability?

2. Methods

2.1. Study sites and data collection

Eddy covariance data between July 1st and December 31st, 2018 from eighteen sites (Table 1), five from Wisconsin (WI) and thirteen from Michigan (MI), were used (Fig. 1). The sites from Wisconsin included a wetland, an agricultural site, and three forest sites; and the sites from Michigan included a wetland, a grassland, eight agricultural sites, a forest, and two urban sites (Table 1). While many of the sites are long-term study sites, six of the sites were instrumented in 2018, and the six-month study period was chosen to maximize the number of active sites. The sites have a variety of instrumentation setups; site-

intercomparisons were performed during an initial QA/QC step, particularly for the six newly instrumented sites in Michigan. Due to data normalization (see below), differences from instrumentation are not expected to add error to the results. The distances between the eighteen sites vary from 10 km to 600 km apart. The time-series surface-atmosphere flux observations used in this study are 30-min net ecosystem exchange (NEE) of carbon, latent heat (LE), sensible heat (H), ecosystem respiration (Reco), gross primary production (GPP), and momentum fluxes (τ). All flux time-series were normalized to be between 0 and 1 in order to detect common frequencies between land-cover types (Greene et al., 2019). τ was quantified using 30-minute air density (ρ) and friction velocity (u^*).

$$\tau = \rho \cdot u^{*2} \tag{1}$$

Surface-atmosphere flux data was processed using a combination of eddy4R (Metzger et al., 2017), EddyPro (Biosciences, 2017) and TK3 Eddy-Covariance Software Package (Mauder and Foken, 2015; Berger et al., 2001) for Wisconsin sites, and a combination of EdiRe (Clement, 1999) and EddyPro for the Michigan sites. NEE from all sites was partitioned into GPP and $R_{\rm eco}$ using REddyProc (Wutzler et al., 2018). Data from one of the Wisconsin sites (Park Falls) was collected hourly, so data were rescaled to 30-minute. Outliers at \pm 3 scaled median absolute deviations from the median were removed for all fluxes. Non-gap-filled data were used for analysis in this work, with gap-filled data from REddyProc analyzed only to quantify the impact of gap-filling on results and are shown only in Table 2.

2.2. Analytical processes

In order to quantify inter-site coherence of surface-atmosphere fluxes, time-series correlation coefficients were calculated between each site-pair – a total of 153 site-pairs for each of the six surface-atmosphere fluxes. Then, the spatial distance in km between each site-pair was calculated. This coherence correlation coefficient of each site-pair was plotted as a function of that site-pairs' geospatial distance, i.e. known as a geostatistical semivariogram diagram. A spherical model was used to quantify the nugget (the intrinsic coherence at zero distance), sill (the minimum average coherence value), and range (the spatial distance where coherence is no longer a function of distance) for each of the six surface-atmosphere fluxes.

Empirical Orthogonal Function (EOF) methods, also known as geographically weighted Principal Component Analysis, were used to decompose the time-series data into orthogonal base functions to quantify common spectral frequencies of spatiotemporal covariation with the larger flux data. With 6 months of data included in this study, frequencies out to ~10 months are quantified, which is well below the Nyquist (or folding) frequency for the data. Due to computational limits, EOFs were calculated independently for the WI and MI clusters, with all data gaps set to zero (Greene et al., 2019). Spatial arrays for both clusters were created with 0.01° latitude and longitude precision, between 41° and 43° N latitude, and 87° and 83° W longitude for Michigan and 44° and 47° N latitude, and 89° and 91° W longitude for Wisconsin. Data was then detrended in time, and the top three modes of variability, as well as their variance percentage for each mode, for each surface-atmosphere flux were computed following the methods of Greene et al. (2019). Anomaly and frequency plots were created on the principal component variables. All analysis was performed in MATLAB R2019a.

3. Results

3.1. Spatial coherence in fluxes

Coherence of NEE directly outside of the footprint of the average site was 92% (Table 2, Fig. 2). Coherence decreased steadily with distance to 58% at a spatial range of 42 km (Table 2, Fig. 2) and on

Table 1
Site information for 18 eddy covariance sites included in this study. Wisconsin (WI) data server (https://flux.aos.wisc.edu/data).

Site information					
Site (Ameriflux site code)	Land-cover type	Cluster	Data availability DOY, DOI	Latitude Longitude	
Lost Creek (US-Los)	Wetland	Wisconsin	182-365, 10.17190/AMF/1246071	46.0827°N 89.9792°W	
Park Falls (US-PFa)	Tall-Tower	Wisconsin	182-365, 10.17190/AMF/1246090	45.9459°N	
				90.2723°W	
Sylvania (US-Syv)	Forest	Wisconsin	182-365, 10.17190/AMF/1246106	46.242°N	
				89.3477°W	
Willow Creek (US-WCr)	Forest	Wisconsin	182-365, 10.17190/AMF/1246111	45.8059°N	
				90.0799°W	
Central Sands (US-CS1)	Agriculture	Wisconsin	182-365, 10.17190/AMF/1617710	44.103051°N	
			400.045	89.537855°W	
KBS T1 (US-KM3)	Agriculture	Michigan	182-365	42.446250°N	
KBS T2 (US-KM2)	A ami au leuma	Mishigan	182-365, 10.17190/AMF/1647440	85.310436°W 42.444040°N	
KBS 12 (US-KW2)	Agriculture	Michigan	182-305, 10.1/190/AMF/104/440	42.444040 N 85.309752°W	
KBS T3 (US-KM1)	Agriculture	Michigan	182-365, 10.17190/AMF/1647439	42.437620°N	
RDS 13 (OS RMII)	rigirealture	Michigan	102 000, 10.17170/71111710 17 107	85.328620°W	
KBS T4 (US-KL1)	Agriculture	Michigan	182-365	42.484740°N	
	o .	· ·		85.442162°W	
KBS T5 (US-KL2)	Agriculture	Michigan	182-365, 10.17190/AMF/1644212	42.476670°N	
				85.446792°W	
KBS T6 (US-KL3)	Agriculture	Michigan	182-365, 10.17190/AMF/1647438	42.473500°N	
				85.447470°W	
KBS T7 (US-KM4)	Grassland	Michigan	182-365, 10.17190/AMF/1634882	42.442350°N	
44	_			85.330190°W	
Kellogg Forest (US-KEF)	Forest	Michigan	198-365	42.365961°N	
Allegan (US-ALG)	Wetland	Michigan	189-365	85.352615°W 42.66888°N	
Allegali (US-ALG)	wetiand	wichigan	189-303	42.00888 N 86.022909°W	
Jackson 1	Agriculture	Michigan	182-300	42.25803°N	
buckson 1	rigirealture	Michigan	102 000	84.842792°V	
Jackson 2 (US-JCK)	Agriculture	Michigan	182-365	42.214287°N	
		· ·		84.853891°W	
Battle Creek, MI (US-BC)	Urban	Michigan	182-365	42.322809°N	
				85.187125°W	
East Lansing, MI (US-MSU)	Urban	Michigan	182-317	42.729345°N	
				84.473669°W	

average remained constant at farther spatial distances, with clusters of site-pairs showing coherence clustering at distances >400 km. Initial results revealed that average coherence between urban and vegetated sites was low (\sim 10%), while the urban-urban coherence pair was close to 100%. Consequently, both urban sites were removed from further analysis as they exhibited fundamentally different time-series characteristics compared to vegetated sites.

Surface-atmosphere fluxes of NEE, GPP, $R_{\rm eco}$, and H showed similar low average range value of 37 km (Fig. 2, Table 2). NEE, GPP, and $R_{\rm eco}$ showed similar sill values of 0.61, while H, LE and τ showed similar lower average value of 0.40. With the exception of τ , all fluxes displayed nugget values of > 0.90. Data analysis between gap-filled and non-gap-filled data is shown in Table 2 to quantify the impact of gap-filling. Results from gap-filled data were similar, with model fits showing large differences in spatial ranges for NEE and LE only. The range for NEE and LE decreased from 42 km to 21 km, and from 130 km to 29 km, respectively, when gap-filled data instead of non-gap-filled were used. Gap-filling did not significantly impact sill or nugget values.

Semivariogram model fits are shown for all surface-atmosphere fluxes for both all distances per each flux (Fig. 3) as well as for the first 150 km (Fig. 4). Over this range, it becomes apparent how dissimilar τ fluxes are to the other surface-atmosphere fluxes, with a higher range and lower nugget and sill values. LE displays a higher range, but similar nugget and sill values to the other land-surface fluxes; the carbon fluxes are, by and large, most similar among each other. Overall, coherence between fluxes are high (>80%) within $\sim\!\!10$ km, and fluxes between site-pairs are strongly connected to the spatial distance between the sites.

3.2. Temporal variability in fluxes

For both clusters of sites, the 1^{st} EOF mode of variability was the dominant mode that explains 78% of the variance (Table 3). Variance in the first mode for τ fluxes was the lowest, but still averaged $\sim\!60\%$. WI sites had lower variance explained in the first mode. The 2^{nd} and 3^{rd} modes of variability correlated to 15% and 7% of the variance, respectively, with τ variance being the highest.

Spectral frequencies for the first principal component for both clusters are shown in Fig. 5. As analysis was done on 30-minute data, a diel frequency is the dominant signal in all flux signals except in Reco. For the majority of fluxes the first harmonic of a diel frequency at 12hours is also observed, which this frequency is strongest in H, LE and τ , and present in NEE and GPP. Fig. 5 subplots (b,d,f,h,j,k) show the same spectral frequencies, rescaled from 2-day to 6-month frequencies. Here, when the diel and harmonic frequencies are removed from the signal, the dominant frequencies for all fluxes occur at around 6-months and capture the seasonal pattern from summer into winter. NEE and GPP have limited component frequencies in-between diel and 6-months, while R_{eco} shows small components at around 2 weeks and 1 month. H, LE and τ fluxes have a much higher relative amount of signal in-between diel and 6-month frequencies, with H having a higher amount of contribution at 2-week than 6-months. The differences between MI and WI clusters are small, once data is rescaled, although the number of WI samples were fewer.

We show the first mode of detrended surface-atmosphere flux variance plotted in Fig. 6 for MI and WI time-series. One clear pattern that emerged was a strong linear temporal trend in GPP and LE in the

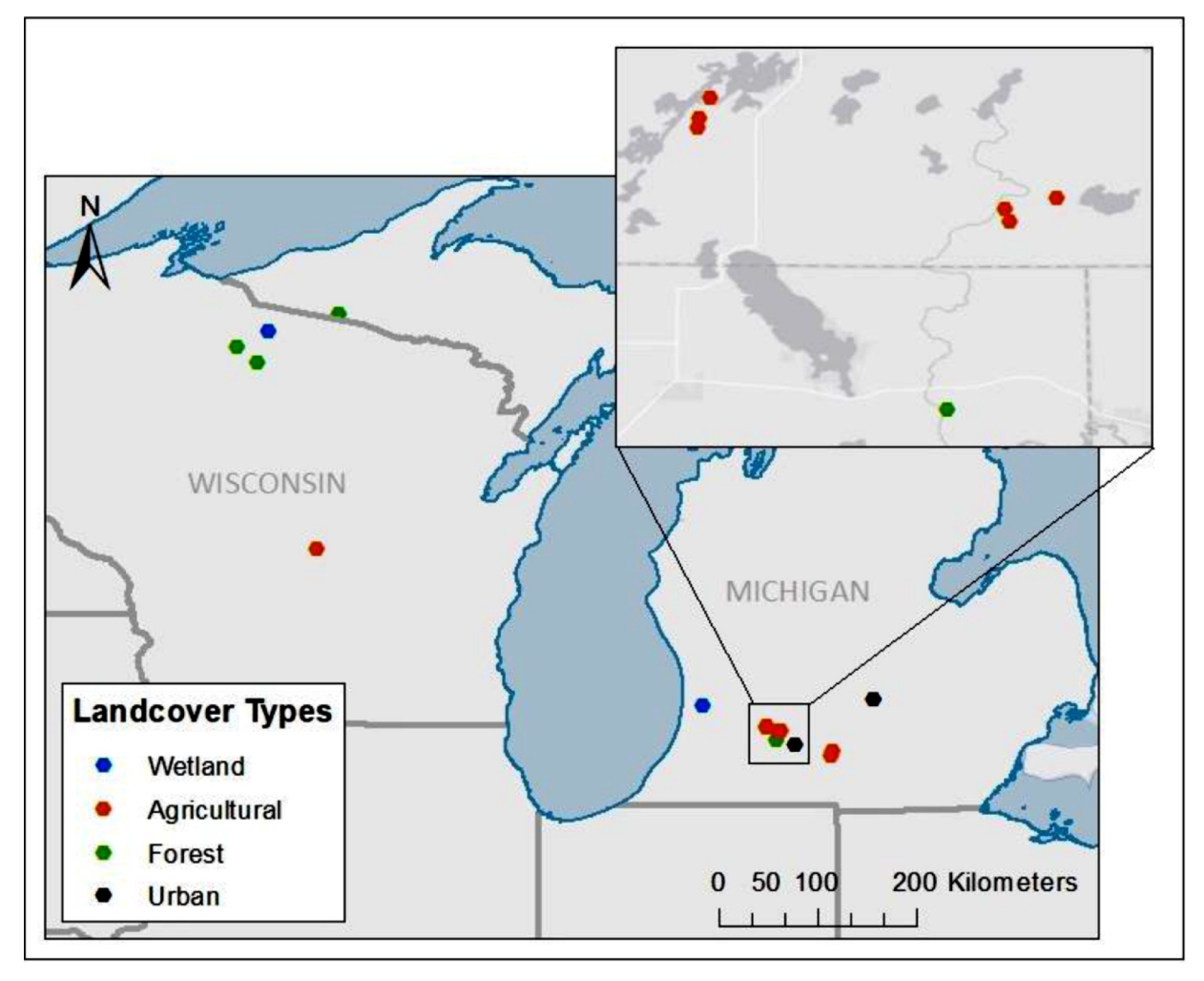


Fig. 1. Location of 18 flux towers in Michigan (MI) and Wisconsin (WI), coded by land-cover type.

 $\label{eq:continuous} \begin{tabular}{ll} Table 2 \\ Data analysis between gap-filled and non-gap-filled spherical fit semivariogram results (range, sill and nugget) for NEE, GPP, Reco, H, LE, <math>\tau$ fluxes.

	Non gap-filled	fluxes		Gap-filled fluxes					
	Range (km)	Sill	Nugget	Range (km)	Sill	Nugget			
NEE	42.10	0.58	0.92	21.32	0.46	0.85			
GPP	33.62	0.62	0.98	38.22	0.72	0.96			
R_{eco}	30.47	0.62	0.92	31.65	0.60	0.92			
H	41.50	0.40	0.97	31.43	0.58	0.87			
LE	130.94	0.44	0.90	29.43	0.57	0.90			
τ	129.36	0.36	0.76	115.27	0.36	0.76			

transition from summer to winter. This linear trend is present but less strong in NEE and $R_{\rm eco}$ as well. Within this subset of fluxes, NEE shows the earliest temporal switch between positive and negative solutions to the EOF, followed temporally by GPP and then both LE and $R_{\rm eco}.$ As noted in the spectral frequencies (Fig. 5), $R_{\rm eco}$ had a limited diel frequency component. Here, that is shown as smaller amount of daily variance in the EOFs. Variance in $\tau,$ and to a smaller extent in H, is without a temporal trend throughout the entire time-series.

Finally, in order to show the geospatial coherence, the semivariogram range results from carbon, H, LE and τ fluxes are presented in Fig. 7. Distances are shown without quantifying areas of overlap between > 2 sites, which would be a factor in the middle of both field site clusters.

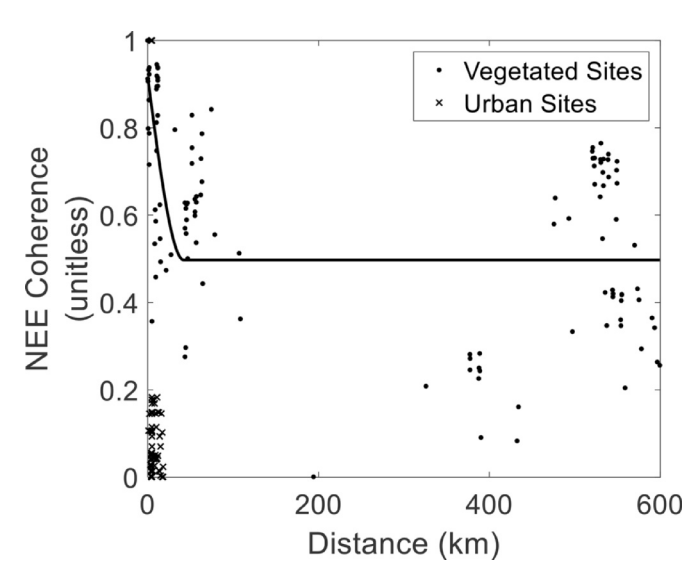


Fig. 2. Spherical fit semivariogram results and site-pair data for NEE fluxes from all possible site-pairs, with site-pairs that include an urban site shown but separate from semivariogram fit.

4. Discussion

The first objective of this work was to determine if surface-atmosphere fluxes are coherent between sites. Strong coherence would

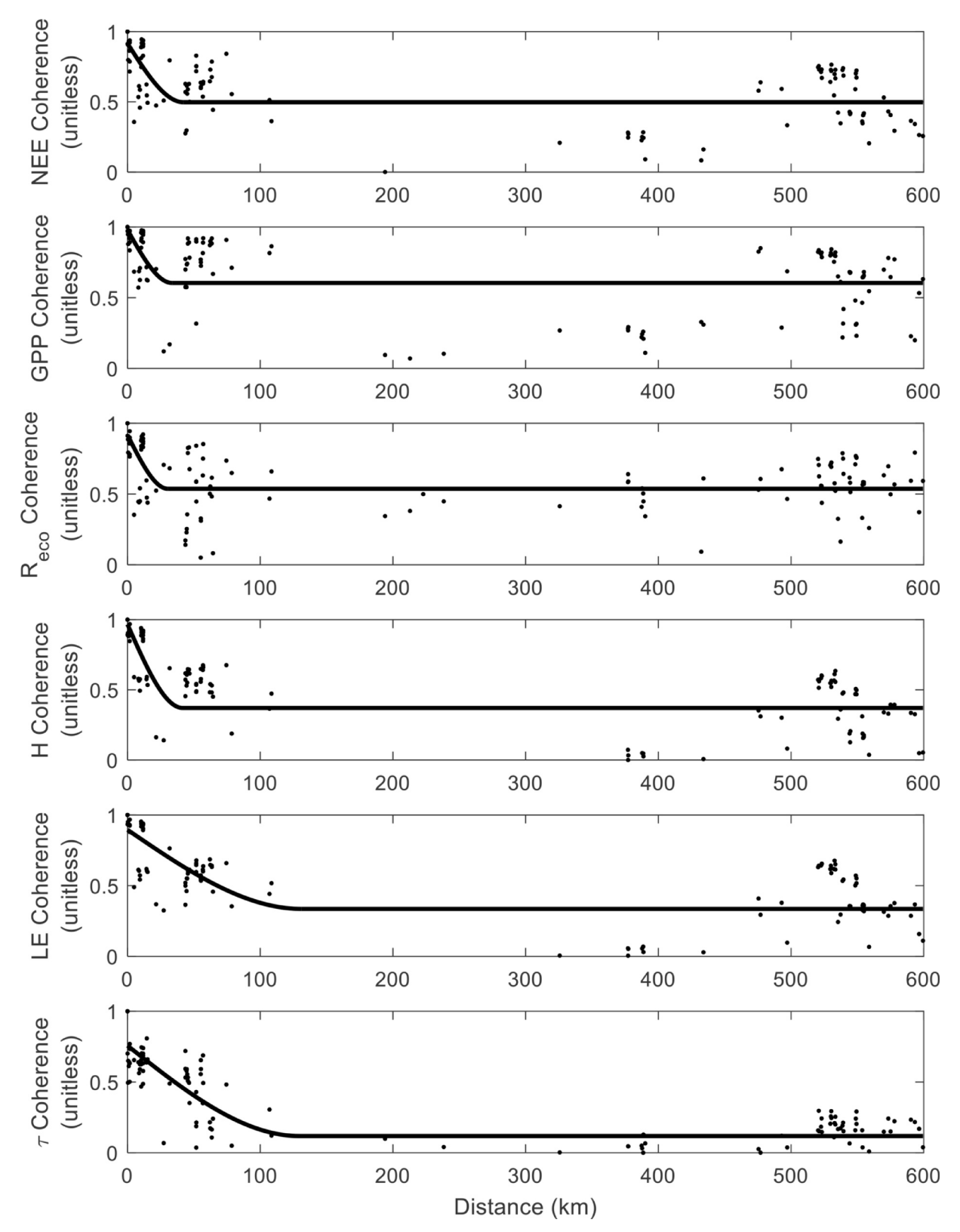


Fig. 3. Spherical fit semivariogram results and site-pair data for NEE, GPP, R_{eco} , H, LE, τ fluxes from vegetated site-pairs.

suggest ecosystem processes have similarities in time and space while weaker coherence would suggest greater fine scale spatial variations in fluxes and the processes that control fluxes, making extrapolation more difficult and uncertain. Using eighteen sites, we showed there is a strong coherence between terrestrial ecosystems at range of 100 - 600 km. Similar results were shown by Hollinger et al. (2004) who used two

forest sites 775 m apart, but our work suggests that these patterns translate across ecosystem types. Using aerodynamic canopy height derived from surface-atmosphere fluxes, Chu et al. (2018) found coherence behavior in 69 forested and 23 grassland sites, showing large-scale and time-varying behaviors between similar land cover types. However, we have found few studies in the literature that directly

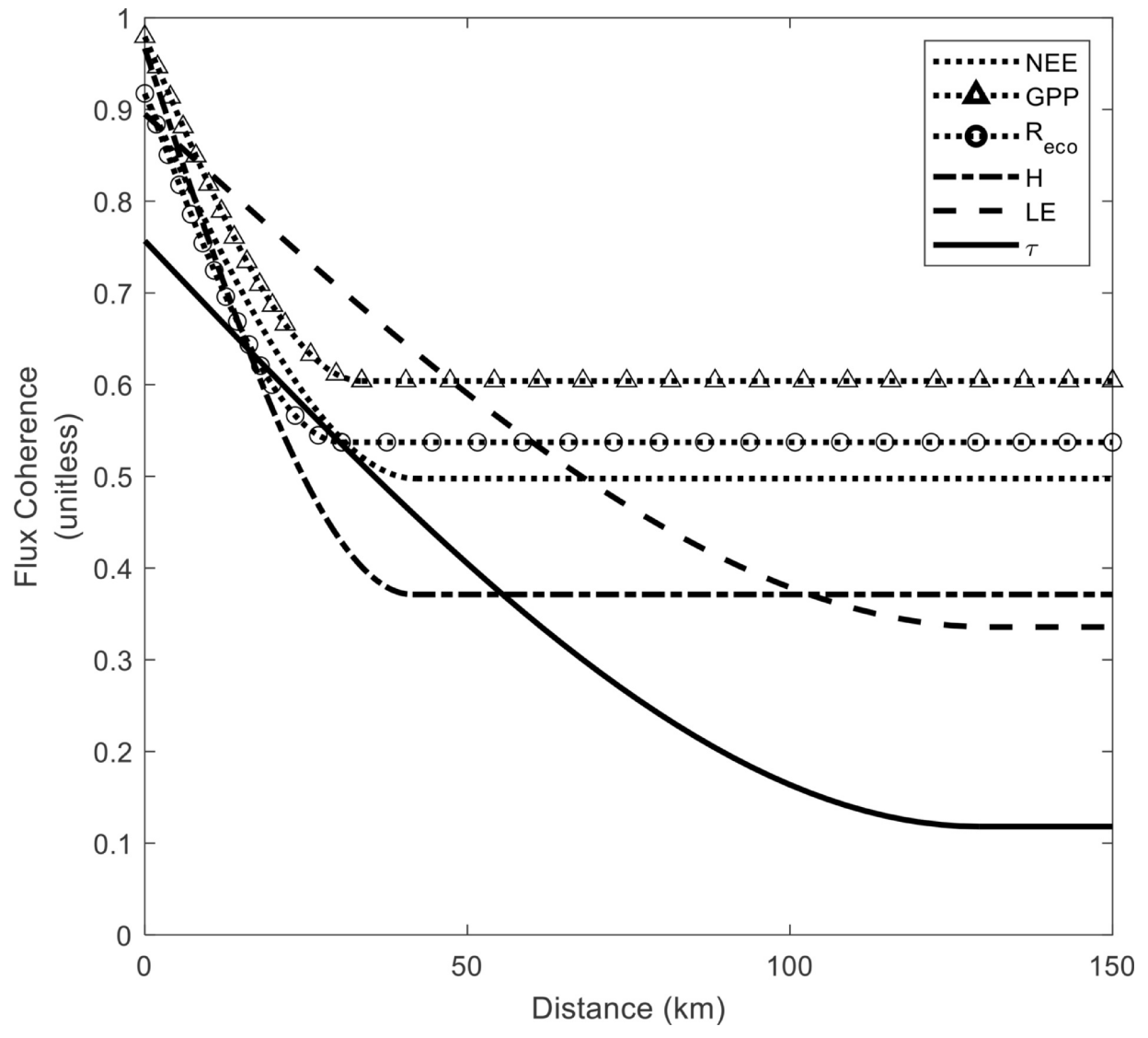


Fig. 4. Spherical fit semivariogram results for NEE, GPP, R_{eco}, H, LE, τ fluxes shown for distances up to 150 km.

Table 3

Percent (%) of variability for highest three Empirical Orthogonal Function (EOF) modes for all surface-atmosphere fluxes, shown for both Michigan and Wisconsin clusters.

Flux	NEE		GPP		Reco		Н		LE		τ		Average
Cluster	MI	WI	MI	WI	MI	WI	MI	WI	MI	WI	MI	WI	
1 st EOF 2 nd EOF 3 rd EOF	79.3 18.1 2.7	82.0 12.6 5.5	87.4 8.4 4.2	84.3 11.4 4.3	79.2 13.4 7.4	60.8 27.3 11.8	95.4 2.6 2.0	78.5 12.4 9.0	95.9 2.8 1.4	71.9 15.6 12.5	63.7 27.8 8.5	55.0 24.9 20.1	77.8 14.8 7.4

quantify the coherence of surface-atmosphere flux.

Notably, within the procedure of quantifying coherence, data from each site was normalized in order to access the temporal correlation so that two sites with a large expected difference in flux magnitude on daily or seasonal time-scales could still be highly coherent. Reed et al. (2018b) showed that non-flux information can be drawn from the time-series characteristics of energy fluxes, such as degree of an ongoing disturbance or long-term water table depth variations. The information within the time-series is lost when observations are summed or averaged over time. Related to this issue, normalizing time-series data in this fashion removes majority of inter-site biases due to instrumental or processing difference. Data in this work has a diverse

set of sensors and processing procedures but few, if any, errors from those differences carry over into these results. In our study, amplitude information from the time-series is lost during normalization. Yet it should be noted that while sites are shown to behave in a coherent fashion at large geospatial scales, the absolute magnitude of fluxes could still be different. Time-series variation is critical for specifying spatial scale of surface-atmosphere upscaling or specifying auto-correlation and geostatistical relationships necessary for deriving sources and sinks from atmospheric tracer-transport inversion (Michalak et al., 2004).

Notably, there existed a clear bifurcation in coherence and behavior between urban and vegetated sites. Within urban sites, long term

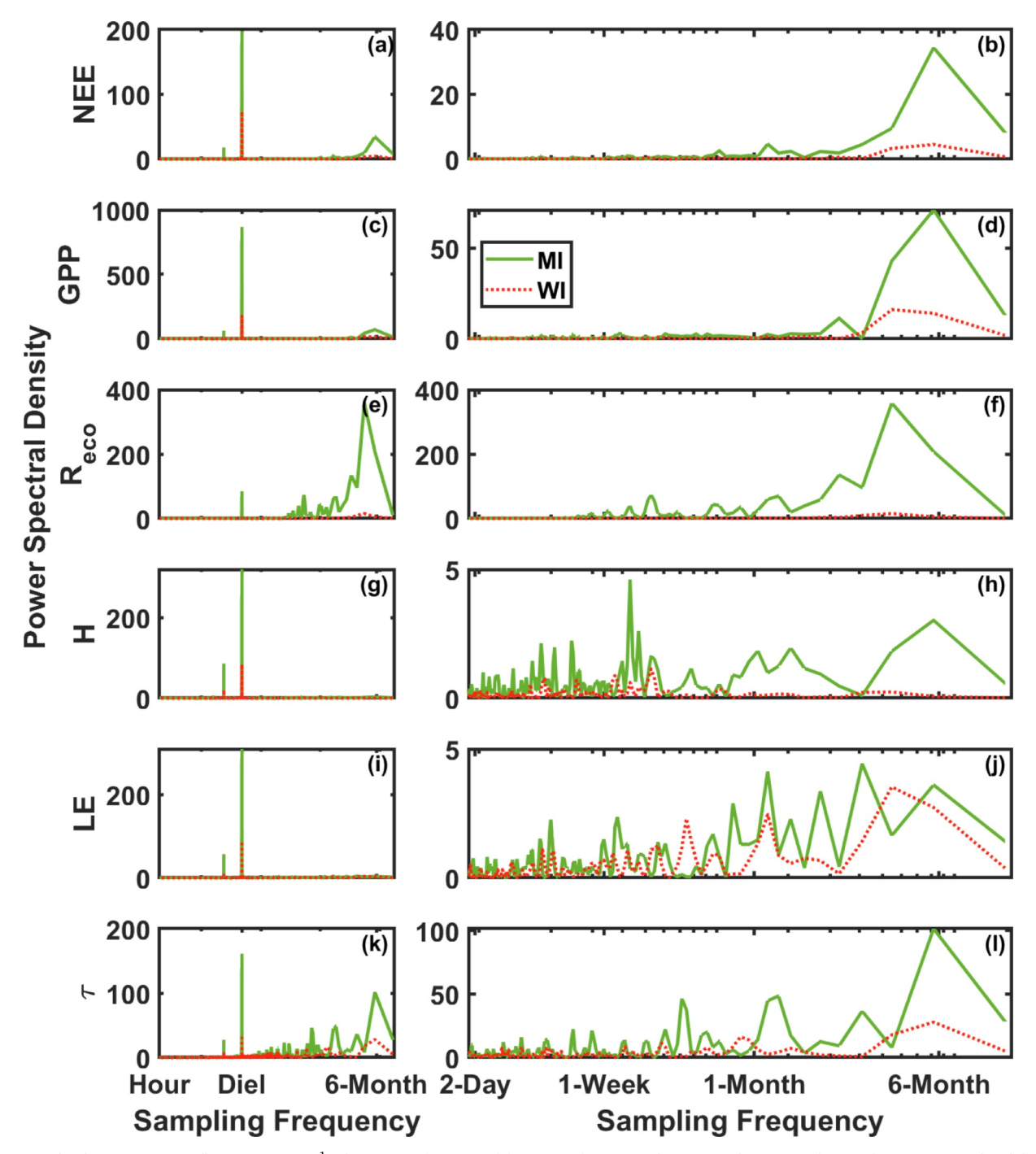


Fig. 5. Spectral coherence power [flux 30-minutes $^{-1}$] shown as a function of frequency for NEE (a,b), GPP (c,d), Reco (e,f), H (g,h), LE (i,g), and τ (k,l) fluxes. Spectral power shown both for the entire frequency range (a,c,e,g,i,k) and only from 2-day frequencies and higher (b,d,f,h,g,l). Data from MI cluster (green) and WI cluster (dashed, red) both shown. (For interpretation of the references to color in this figure legend, the reader is referred to the web version of this article.) .

records have shown flux differences between urban and vegetation sectors of a single flux footprint (Vesala et al., 2008), highlighting the differences between vegetation and non-vegetation land-surface types. Velasco and Roth (2010) found a strong signal from vehicular traffic within urban sites, while daytime carbon fluxes were connected to the spatial extent of vegetation at suburban sites. In general, urban and vegetated sites are shown here and throughout literature to have divergent characteristics implying a difference set of land-surface processes that control and regulate fluxes.

Similarly, we have not included open-water fluxes in these results due to the differences in controlling time-scales of water-column fluxes. Reed et al. (2018a) showed lake-atmosphere fluxes to have a significant

2-week and 1-month frequency component, as well as a reduced diurnal signal. In this study, we included two wetland sites because they have similar time-series modes of variability, but we do not suggest terrestrial fluxes could be used to estimate fluxes from open-water. This is evident in Fig. 7 where open water areas are masked.

Our results might not apply to model parameters (e.g., maximum photosynthesis rates or phenological data) over similar geospatial scales. Hollinger et al. (2004) using a pair of forested sites <1 km apart and found model parameters not vary from one to another site. However, at larger geospatial scales with multiple plant functional types, Xiao et al. (2011) found parameters from a single site are not representative of the plant functional type at regional scales. Parameters

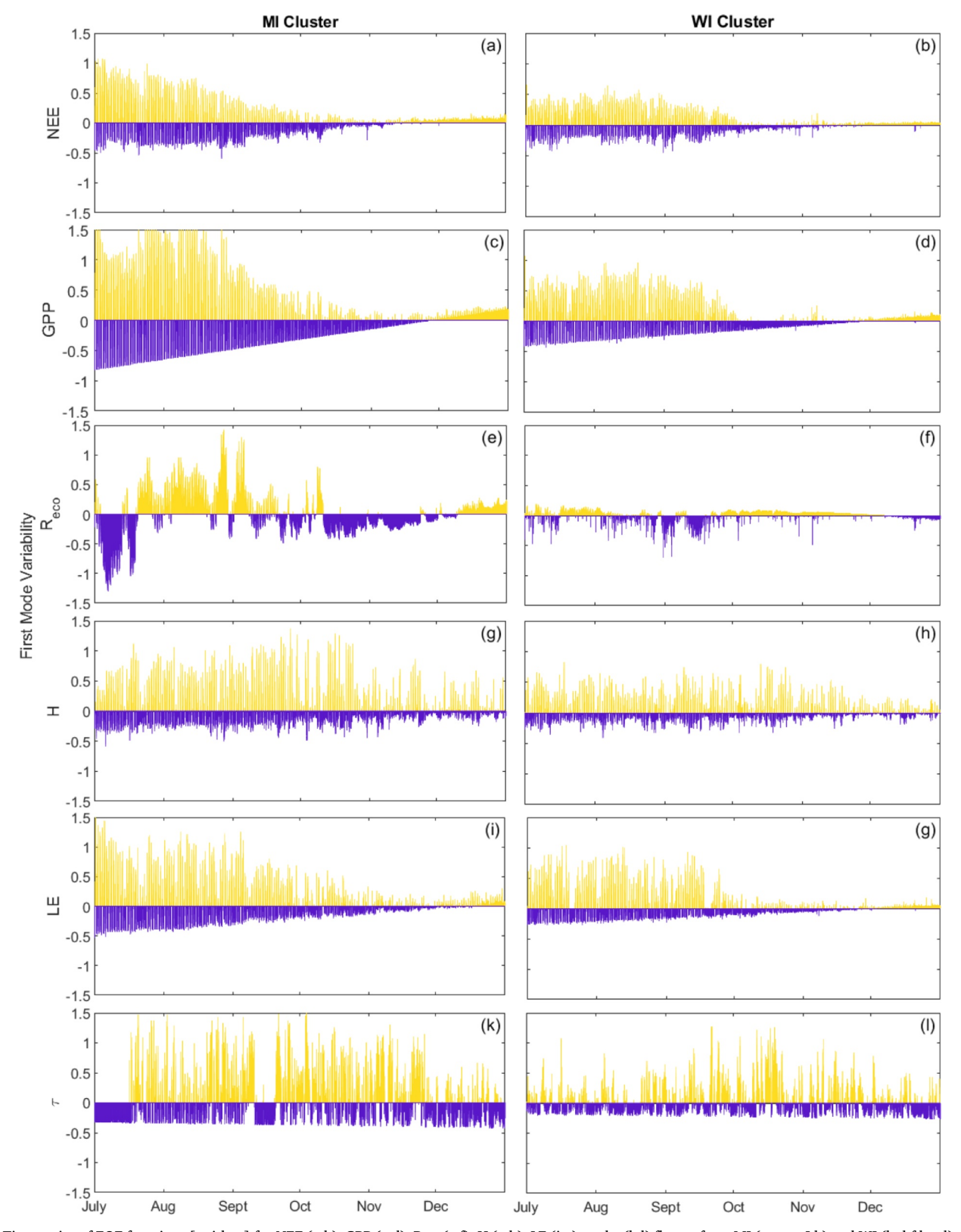


Fig. 6. Time-series of EOF functions [unitless] for NEE (a,b), GPP (c,d), R_{eco} (e,f), H (g,h), LE (i,g), and τ (k,l) fluxes, from MI (a,c,e,g,I,k) and WI (b,d,f,h,g,l) clusters over the six-month study period. Both positive (yellow) and negative (purple) orthogonal solutions shown. (For interpretation of the references to color in this figure legend, the reader is referred to the web version of this article.).

and estimates are improved when using multi-sites with similar plant functional types. In sum, the lack of extrapolating from one to another site on a larger geospatial scale could lead to high levels of uncertainties in regional flux estimates (Xiao et al., 2011) in addressing the issue of

how fluxes and flux based parameters can be estimated accurately is an ongoing area of research, particularly at what spatial scales results from one site can be applied to another site.

Once we address if surface-atmosphere fluxes can be spatially

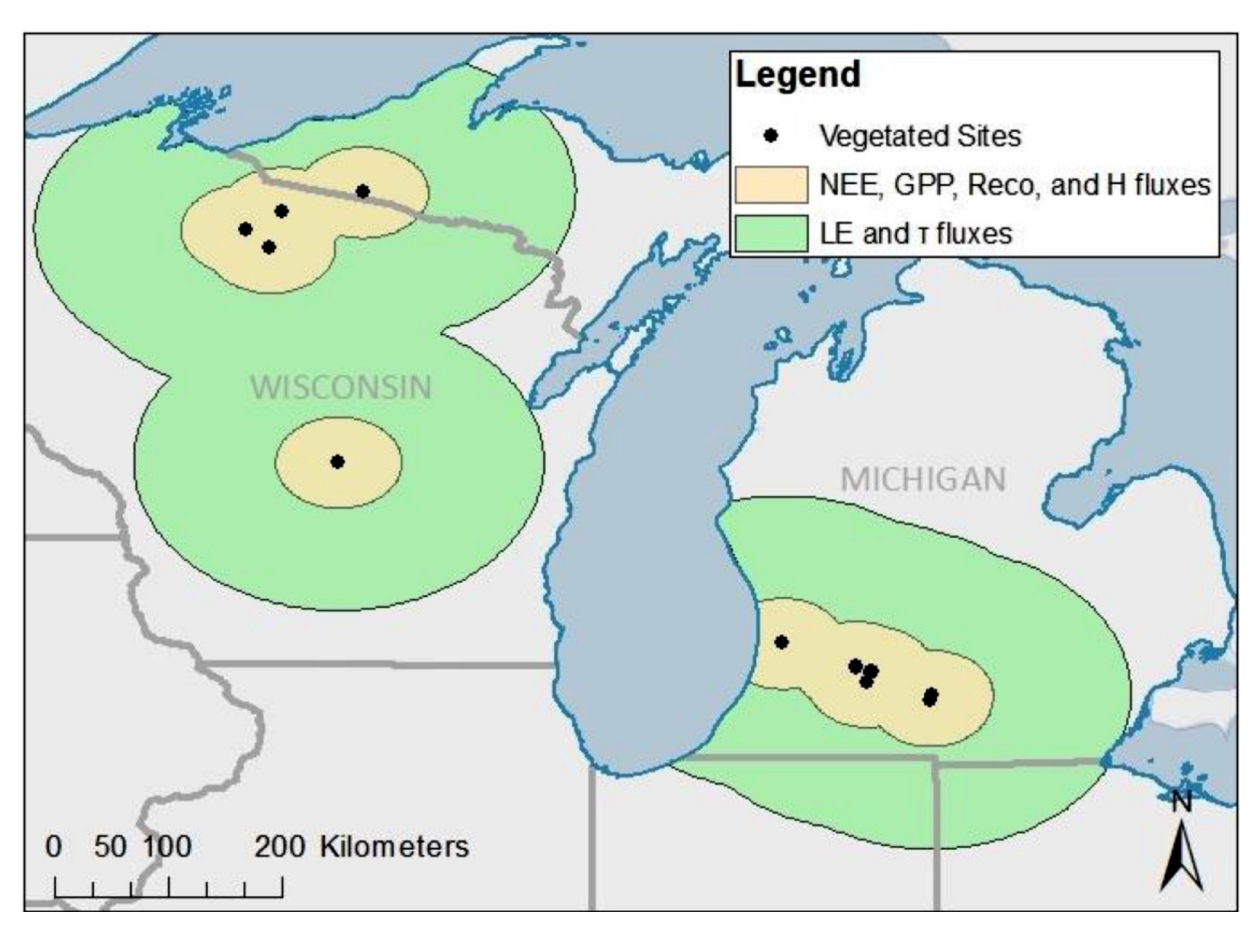


Fig. 7. Site map of vegetated field sites in Michigan (MI) and Wisconsin (WI). Spatial zone of coherence for carbon cycling and H fluxes shown in tan, for LE and τ fluxes shown in green. (For interpretation of the references to color in this figure legend, the reader is referred to the web version of this article.).

coherent among multiple sites, the follow-up question of what range fluxes can be coherent can be answered. With two of the highest density clusters of flux sites, we are able to show for the first time that there is a relationship between fluxes across the landscape at scales of $\sim\!100$ km. We show that directly outside of flux footprints, fluxes are highly coherent, up to 95%. Flux coherence decreases down to 56-40% coherence at distances of $>\!100$ km, where coherence is relatively stable across the study region.

At small spatial scales, flux coherence has been studied in the literature. Using a single forested site-pair ~775 m apart, Hollinger et al. (2004) found a strong signal coherence between air temperature, solar radiation and carbon fluxes. Radiation had high inter-site coherence (>0.95 coherence) at periods below ~4 hours, with air temperature and NEE having similarly high coherence at periods of below \sim 3 hours, showing that over <1 km, fluxes are strongly coherent for multiple hours. With a spatially dense field campaign, Ge et al. (2015) and Liu et al. (2016) used area-to-area regression Kriging from 17 field sites to upscale EC measurement to measurement scales on the order of large aperture scintillometer observations. With study region of 5.5 km by 5.5 km, Ge et al. (2015) reported variogram derived ranges of \sim 3 km. This is a smaller distance than what we found, potentially due to a smaller number of land-cover types, with 14 of 17 of Ge et al. (2015) being corn sites, where 8 of our sites were agricultural land-cover, but with 4 different crop types. Based on the same field campaign, Li et al. (2018) scaled evapotranspiration observations to the scale of MODIS pixels using six different scaling approaches, and concluded that for moderately heterogeneous surfaces, Kriging methods similar to methods in this work produced the best scaling results.

Through spectral analysis, we show common frequencies of variability for the land-surface fluxes used in this study. It is not surprising

that over the 6-month study period, diel patterns dominate the spectral signal. This is the frequency that matches primarily that of solar radiation, which in turn drives environmental temperatures, GPP and heat flux signals (Ouyang et al., 2014). Using wavelet analysis from two forested sites, Stoy et al. (2005) found strong diel signals for radiation, temperature, and NEE. However, there are secondary harmonic signals present at higher frequencies as well since surface-atmosphere fluxes are not perfect sine waves with equally negative magnitudes at night relative to daytime fluxes (Boland, 1995; Robinson and Treitel, 2000). Typical ecosystem fluxes are approximately constant at night, either near zero for H and LE, or positive for NEE (with partitioned GPP and Reco fluxes near zero as well) (Campbell and Norman, 2012). In order to match the harmonic-sine wave observations, the EOF analysis found high amounts of common variability at the 2nd and 3rd harmonics of the diel frequency, i.e. 12-hours and 6-hours. In short, surface-atmosphere fluxes are dominated by diel patterns, and any other mode of variability at higher frequencies builds on top of the diel signal.

The EOF frequencies from ecosystem respiration have a very weak diel signal, coupled with the strongest seasonal pattern. While this could be influenced by the respiration partitioning model used here and its inputs, this is similar to Stoy et al. (2005) who found ecosystem respiration to be sensitive to the drivers that act on weekly and monthly time scales. Environmental temperature at short time-scales explained respiration variability, but energy transfer through ecosystem needs to account for energy storage (Meyers and Hollinger, 2004), time lags (Reed et al., 2018b), and variable heat capacity (Ochsner et al., 2007). EOF's frequencies are derived from the observational land-surface flux time-series themselves, and it is important to note the respiration driver time-series of environmental temperature or moisture availability were not a part of the EOF input. The resulting respiration frequencies were

derived only from the respiration observations.

At frequency of >24 hours, modes of variability show divergent behavior between fluxes. The non-carbon fluxes (H, LE, τ) showed significant signal strength between sub-weekly and sub-seasonal timescales, with H having a ~10-day frequency signal and LE having a ~1 month and ~4 month signals that are stronger than their seasonal signals. At these time-scales, ecological responses to environmental changes often dominate flux variability. Richardson et al. (2007) found that at increasing larger time-scales - days to months to years - variation in environmental drivers matter less as ecosystems response to changing conditions becomes increasingly important. At annual scale, 40% of the variance in modeled NEE was from environmental forcing. and 55% from biotic response variation to this forcing. Similarly, Katul et al. (2001) found canopy physiology and structure dynamics at monthly time-scales to be the connection between surface-atmosphere fluxes and environmental drivers. This pattern is also seen in results from Fig. 6, where carbon (NEE and GPP) and LE fluxes show a seasonal trend within their EOF time-series. We interpret this pattern as the impact of monthly-to-seasonal scale changes in biological responses to environmental drivers, here noted across large geospatial scales between the MI and WI site clusters. Using species-specific models, phenology can be scaled from local to regional spatial scales with a high degree of accuracy (Chuine et al., 2000; Cleland et al., 2007). Here, we suggest surface-atmosphere fluxes can be scaled regionally following similar principles.

5. Conclusions

While several studies have utilized spatially dense clusters of surface-atmosphere flux observations, this work is the first to explicitly quantify the extent and magnitude of coherent behavior of surface fluxes. By quantifying this coherence, we demonstrate that the degree to which ecosystems outside of the footprint of a single flux tower behave similar to observations within the footprint. Our spatial coherence is for re-scaled flux data; however, our findings show that surface-atmosphere fluxes are coherent when land-cover differences are normalized. This suggests that fluxes from one ecosystem potentially can be used to estimate fluxes from similar ecosystems. If differences between ecosystem or land-cover type are quantified, fluxes from a single site can be scaled across the entire landscape.

Scaling EC surface-atmosphere fluxes became an active area of research as soon as the observational technique became widely adopted. The fundamental mismatches between flux footprint scales and remote sensing or modeling pixels can be directly addressed if observational fluxes are to be extrapolated beyond the flux footprint. Ultimately, a single surface-atmosphere flux observational record could be scaled beyond the observation's footprint to the entire landscape, fundamentally increasing the power of flux observations and transforming how flux data is scaled up.

Declaration of Competing Interest

The authors declare that they have no known competing financial interests or personal relationships that could have appeared to influence the work reported in this paper.

Acknowledgments

JC, MA, and DER collected MI data, ARD collected WI data. DER processes fluxes for all sites. JP did data analysis. JP and DER wrote the first draft of the manuscript and all authors contributed to editing the paper. This material is based upon work supported in part by the NASA Carbon Cycle & Ecosystems program (NNX17AE16G); the Great Lakes Bioenergy Research Center funded by the U.S. Department of Energy, Office of Science, Office of Biological and Environmental Research

under Award Numbers DE-SC0018409 and DE-FC02-07ER64494; and the Long-term Ecological Research Program (DEB 1637653) at the Kellogg Biological Station. ARD acknowledges support from the DOE Ameriflux Network Management Project award to the ChEAS core site cluster, the Wisconsin Dept of Natural Resources, the Wisconsin Potato and Vegetable Growers Association, and the NSF North Temperate Lakes Long Term Ecological Research (NTL-LTER) award #DEB-1440297. We would like to acknowledge Yost R. for helping with geospatial statistics.

References

- Badeck, F.W., Bondeau, A., Bottcher, K., Doktor, D., Lucht, W., Schaber, J., Sitch, S., 2004.
 Responses of spring phenology to climate change. New Phytol. 162, 295–309.
- Baldocchi, D., 2014. Measuring fluxes of trace gases and energy between ecosystems and the atmosphere-the state and future of the eddy covariance method. Glob. Change Biol. 20, 3600-3609.
- Baldocchi, D.D., Luxmoore, R.J., Hatfield, J.L., 1991. Discerning the forest from the trees an essay on scaling canopy stomatal conductance. Agric. For. Meteorol. 54, 197–226.
- Barcza, Z., Kern, A., Haszpra, L., Kljun, N., 2009. Spatial representativeness of tall tower eddy covariance measurements using remote sensing and footprint analysis. Agric. For. Meteorol. 149, 795–807.
- Berger, B.W., Davis, K.J., Yi, C.X., Bakwin, P.S., Zhao, C.L., 2001. Long-term carbon dioxide fluxes from a very tall tower in a northern forest: flux measurement methodology. J. Atmos. Ocean. Technol. 18, 529–542.
- Beyrich, F., Herzog, H.J., Neisser, J., 2002. The LITFASS project of DWD and the LITFASS-98 experiment: the project strategy and the experimental setup. Theor. Appl. Climatol. 73. 3–18.
- Beyrich, F., Leps, J.P., Mauder, M., Bange, J., Foken, T., Huneke, S., Lohse, H., Ludi, A., Meijninger, W.M.L., Mironov, D., Weisensee, U., Zittel, P., 2006. Area-averaged surface fluxes over the litfass region based on eddy-covariance measurements. Bound. Laver Meteorol. 121, 33–65.
- Beyrich, F., Mengelkamp, H.-T., 2006. Evaporation over a heterogeneous land surface: EVA_GRIPS and the LITFASS-2003 experiment—an overview. Bound. Layer Meteorol. 121, 5–32.
- Billesbach, D., Fischer, M., Torn, M., Berry, J., 2004. A portable eddy covariance system for the measurement of ecosystem–atmosphere exchange of CO2, water vapor, and energy. J. Atmos. Ocean. Technol. 21, 639–650.
- Biosciences, L., 2017. EddyPro Software Instruction Manual. LI-COR Inc., Lincoln, Nebraska, USA.
- Boland, J., 1995. Time-series analysis of climatic variables. Sol. Energy 55, 377–388.Bonan, G.B., 1995. Land atmosphere interactions for climate system models coupling biophysical, biogeochemical, and ecosystem dynamical processes. Remote Sens. Environ. 51, 57–73.
- Bounoua, L., Defries, R., Collatz, G.J., Sellers, P., Khan, H., 2002. Effects of land cover conversion on surface climate. Clim. Change 52, 29–64.
- Campbell, G.S., Norman, J.M., 2012. An Introduction to Environmental Biophysics. Springer Science & Business Media.
- Chu, H.S., Baldocchi, D.D., Poindexter, C., Abraha, M., Desai, A.R., Bohrer, G., Arain, M.A., Griffis, T., Blanken, P.D., O'halloran, T.L., Thomas, R.Q., Zhang, Q., Burns, S.P., Frank, J.M., Christian, D., Brown, S., Black, T.A., Gough, C.M., Law, B.E., Lee, X., Chen, J.Q., Reed, D.E., Massman, W.J., Clark, K., Hatfield, J., Prueger, J., Bracho, R., Baker, J.M., Martin, T.A., 2018. Temporal dynamics of aerodynamic canopy height derived from eddy covariance momentum flux data across North American flux networks. Geophys. Res. Lett. 45, 9275–9287.
- Chuine, I., Cambon, G., Comtois, P., 2000. Scaling phenology from the local to the regional level: advances from species-specific phenological models. Glob. Change Biol. 6, 943–952.
- Cleland, E.E., Chuine, I., Menzel, A., Mooney, H.A., Schwartz, M.D., 2007. Shifting plant phenology in response to global change. Trends Ecol. Evol. 22, 357–365.
- Clement, R., 1999. EdiRe Data Software, v. 1.5. 0.32. University of Edinburgh, Edinburgh, UK.
- Desai, A.R., 2010. Climatic and phenological controls on coherent regional interannual variability of carbon dioxide flux in a heterogeneous landscape. J. Geophys. Rese.-Biogeosci. 115.
- Desai, A.R., Noormets, A., Bolstad, P.V., Chen, J., Cook, B.D., Davis, K.J., Euskirchen, E.S., Gough, C., Martin, J.G., Ricciuto, D.M., 2008. Influence of vegetation and seasonal forcing on carbon dioxide fluxes across the Upper Midwest, USA: implications for regional scaling. Agric. For. Meteorol. 148, 288–308.
- Ge, Y., Liang, Y.Z., Wang, J.H., Zhao, Q.Y., Liu, S.M., 2015. Upscaling Sensible heat fluxes with area-to-area regression Kriging. IEEE Geosci. Remote Sens. Lett. 12, 656–660.
- Greene, C.A., Thirumalai, K., Kearney, K.A., Delgado, J.M., Schwanghart, W., Wolfenbarger, N.S., Thyng, K.M., Gwyther, D.E., Gardner, A.S., Blankenship, D.D., 2019. The climate data toolbox for MATLAB. Geochem. Geophys. Geosyst. 20, 3774–3781.
- Halldin, S., Gryning, S.-E., Gottschalk, L., Jochum, A., Lundin, L.-C., van de Griend, A., 1999. Energy, water and carbon exchange in a boreal forest landscape—NOPEX experiences. Agric. For. Meteorol. 98, 5–29.
- Heinemann, G., Kerschgens, M., 2005. Comparison of methods for area-averaging surface energy fluxes over heterogeneous land surfaces using high-resolution non-hydrostatic simulations. Int. J. Climatol. 25, 379–403.
- Hollinger, D., Aber, J., Dail, B., Davidson, E., Goltz, S., Hughes, H., Leclerc, M., Lee, J.,

- Richardson, A., Rodrigues, C., 2004. Spatial and temporal variability in forest–atmosphere CO2 exchange. Glob. Change Biol. 10, 1689–1706.
- Katul, G., Lai, C.T., Schafer, K., Vidakovic, B., Albertson, J., Ellsworth, D., Oren, R., 2001. Multiscale analysis of vegetation surface fluxes: from seconds to years. Adv. Water Res. 24, 1119–1132.
- Li, X., Liu, S.M., Li, H.X., Ma, Y.F., Wang, J.H., Zhang, Y., Xu, Z.W., Xu, T.R., Song, L.S., Yang, X.F., Lu, Z., Wang, Z.Y., Guo, Z.X., 2018. Intercomparison of six upscaling evapotranspiration methods: from site to the satellite pixel. J. Geophys. Res.-Atmos. 123, 6777–6803.
- Liu, S.M., Xu, Z.W., Song, L.S., Zhao, Q.Y., Ge, Y., Xu, T.R., Ma, Y.F., Zhu, Z.L., Jia, Z.Z., Zhang, F., 2016. Upscaling evapotranspiration measurements from multi-site to the satellite pixel scale over heterogeneous land surfaces. Agric. For. Meteorol. 230, 97–113.
- Mauder, M., Foken, T., 2015. Documentation and Instruction Manual of the Eddy-Covariance Software Package TK3 (update). Univ., Abt. Mikrometeorologie.
- Metzger, S., Durden, D., Sturtevant, C., Luo, H., Pingintha-Durden, N., Sachs, T., Serafimovich, A., Hartmann, J., Li, J., Xu, K., 2017. eddy4R 0.2. 0: a DevOps model for community-extensible processing and analysis of eddy-covariance data based on R, Git, Docker, and HDP5. Geosci. Model Dev. 10, 3189–3206.
- Meyers, T.P., Hollinger, S.E., 2004. An assessment of storage terms in the surface energy balance of maize and soybean. Agric. For. Meteorol. 125, 105–115.
- Michalak, A.M., Bruhwiler, L., Tans, P.P., 2004. A geostatistical approach to surface flux estimation of atmospheric trace gases. J. Geophys. Res. 109.
- Ochsner, T.E., Sauer, T.J., Horton, R., 2007. Soil heat storage measurements in energy balance studies. Agron. J. 99, 311–319.
- Ouyang, Z.T., Chen, J.Q., Becker, R., Chu, H.S., Xie, J., Shao, C.L., John, R., 2014. Disentangling the confounding effects of PAR and air temperature on net ecosystem exchange at multiple time scales. Ecol. Complex. 19, 46–58.
- Ran, Y.H., Li, X., Sun, R., Kljun, N., Zhang, L., Wang, X.F., Zhu, G.F., 2016. Spatial representativeness and uncertainty of eddy covariance carbon flux measurements for upscaling net ecosystem productivity to the grid scale. Agric. For. Meteorol. 230, 114-127.
- Reed, D.E., Dugan, H.A., Flannery, A.L., Desai, A.R., 2018a. Carbon sink and source dynamics of a eutrophic deep lake using multiple flux observations over multiple years. Limnol. Oceanogr. Lett. 3, 285–292.

- Reed, D.E., Frank, J.M., Ewers, B.E., Desai, A.R., 2018b. Time dependency of eddy covariance site energy balance. Agric. For. Meteorol. 249, 467–478.
- Richardson, A.D., Hollinger, D.Y., Aber, J.D., Ollinger, S.V., Braswell, B.H., 2007. Environmental variation is directly responsible for short- but not long-term variation in forest-atmosphere carbon exchange. Glob. Change Biol. 13, 788–803.
- Robinson, E.A., Treitel, S., 2000. Geophysical Signal Analysis. Society of Exploration Geophysicists.
- Sellers, P., Hall, F., Asrar, G., Strebel, D., Murphy, R., 1988. The first ISLSCP field experiment (FIFE). Bull. Am. Meteorol. Soc. 69, 22–27.
- Shuttleworth, W.J., Gurney, R.J., Hsu, A.Y., Ormsby, J.P., 1989. FIFE: the variation in energy partition at surface flux sites. 186. IAHS Publ., pp. 523.
- Stoy, P.C., Katul, G.G., Siqueira, M.B.S., Juang, J.Y., Mccarthy, H.R., Kim, H.S., Oishi, A.C., Oren, R., 2005. Variability in net ecosystem exchange from hourly to interannual time scales at adjacent pine and hardwood forests: a wavelet analysis. Tree Physiol. 25, 887–902.
- Velasco, E., Roth, M., 2010. Cities as net sources of CO₂: review of atmospheric CO₂ exchange in urban environments measured by eddy covariance technique. Geogr. Compass 4 (9), 1238–1259.
- Vesala, T., Järvi, L., Launiainen, S., Sogachev, A., Rannik, Ü., Mammarella, I., Ivola, E.S., Keronen, P., Rinne, J., Riikonen, A., 2008. Surface-atmosphere interactions over complex urban terrain in Helsinki, Finland. Tellus B 60, 188–199.
- Wu, C.Y., Munger, J.W., Niu, Z., Kuang, D., 2010. Comparison of multiple models for estimating gross primary production using MODIS and eddy covariance data in Harvard Forest. Remote Sens. Environ. 114, 2925–2939.
- Wutzler, T., Lucas-Moffat, A., Migliavacca, M., Knauer, J., Sickel, K., Sigut, L., Menzer, O., Reichstein, M., 2018. Basic and extensible post-processing of eddy covariance flux data with REddyProc. Biogeosciences 15 (16), 5015–5030.
- Xiao, J.F., Davis, K.J., Urban, N.M., Keller, K., Saliendra, N.Z., 2011. Upscaling carbon fluxes from towers to the regional scale: Influence of parameter variability and land cover representation on regional flux estimates. J. Geophys. Res.-Biogeosci. 116.
- Xiao, J.F., Ollinger, S.V., Frolking, S., Hurtt, G.C., Hollinger, D.Y., Davis, K.J., Pan, Y.D., Zhang, X.Y., Deng, F., Chen, J.Q., Baldocchi, D.D., Law, B.E., Arain, M.A., Desai, A.R., Richardson, A.D., Sun, G., Amiro, B., Margolis, H., Gu, L.H., Scott, R.L., Blanken, P.D., Suyker, A.E., 2014. Data-driven diagnostics of terrestrial carbon dynamics over North America. Agric. For. Meteorol. 197, 142–157.